An Investigation of S(α ,β) Thermal Scattering Law on Criticality Estimation

Seung Hyoen Choi and Ser Gi Hong*
Department of Nuclear Engineering Hanyang University
colin6648@hanyang.ac.kr; *Corresponding author: hongsergi@hanyang.ac.kr

Keywords: S(α,β), TSL, GBC-32

1. Introduction

In reactor core design and analysis, the S(α, β) thermal scattering law (TSL) has been adopted to consider the energy exchange between neutron and target atoms in the thermal energy range. In criticality safety assessments of spent nuclear fuel dry storage facilities, a conservative approach is employed by evaluating criticality with the storage cask fully flooded with water [1]. This approach necessitates high accuracy in thermal neutron evaluation, requiring the use of cross-section data that incorporates the S(α, β) thermal scattering law (TSL).

This study investigates the impact of applying the S(α,β) on multiplication factor calculations in criticality assessments. We examine how the inclusion or exclusion of TSL affects criticality predictions in spent fuel storage systems. For evaluating the effect of S(α,β), we considered a simple 2D fuel assembly model and the GBC-32 cask. The spent nuclear fuels in the GBC-32 cask were considered with an axial burnup distribution and burnup credit. And the thermal scattering law was applied to the following isotopes: uranium (U) and oxygen (O) in UO_2, and hydrogen (H) and oxygen (O) in H_2O.

2. Codes and Methodology

2.1 Codes

This study employed two Monte Carlo neutron transport codes for core criticality calculations. Serpent2, a continuous-energy Monte Carlo code developed by VTT Technical Research Centre of Finland, was used as the primary calculation tool [2]. For comparison and verification, we utilized MCNP6, a general-purpose, continuous-energy Monte Carlo radiation transport code capable of tracking various particle types across a wide energy range [3]. Both codes utilized the ENDF/B-VII.1 cross-section library for neutron transport calculations. For determining the spent fuel composition in the GBC-32 cask, two modules from the SCALE code system were used.

To calculate the material composition of spent nuclear fuel, we utilized TRITON and ORIGAMI codes. TRITON, a multipurpose control module, performs transport, depletion, and sensitivity and uncertainty analysis. It provides automated cross-section processing and multigroup transport calculations for various geometries, coupled with the ORIGEN depletion module. ORIGAMI computes detailed isotopic compositions for LWR assemblies with UO2 fuel using the ORIGEN transmutation code and pre-generated libraries. It allows for lumped fuel modeling with axial zoning options [4]. These capabilities enabled us to accurately determine the composition of spent nuclear fuel for our analysis.

2.2 Modeling of 2D Fuel Assembly

To investigate the effects of S(α,β), a simple 2D Fuel Assembly (FA) was modeled. As shown in **Fig.1**, the FA follows the Westinghouse 17x17 style assembly design. The dimensional and material information for the FA can be found in Table I. Zircaloy-4 was used for both the cladding material and guide tubes, and the fuel enrichment was set at 5 wt.%. For the purposes of modeling, spacer grids and dimples were ignored. The water density was set at 1 g/cm³.

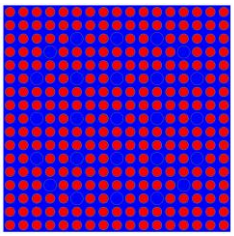

Fig. 1. Figuration of fuel assembly

Table I. Parameters of fuel assembly

Parameters	
Number of fuel rods	264
Number of thimbles	24
Number of Instrument thimbles	1
Guide tube material	Zircaloy-4
Instrument thimble material	Zircaloy-4
Lattice pitch (cm)	1.25984
Fuel Rod Diameter (cm)	0.94996
Pellet Diameter (cm)	0.81915
Diametral Gap (cm)	0.01651
Clad Thickness (cm)	0.05715
Gap material	Helium
Clad material	Zircaloy-4
Density (g/cm3)	10.223
Enrichment	5 wt.%

2.3 Modeling of GBC-32 cask

As shown in **Fig. 2**, to evaluate the effects of S(α, β) in criticality assessments, we created a simplified model of the GBC-32 cask. The dimensional information for the GBC-32 cask can be found in **Table II**. For simplicity, spacer grids and dimples were excluded from the simulation. To calculate the composition of spent nuclear fuel, we used TRITON and ORIGAMI codes. Through these two codes, both axial burnup distribution and compositions for each axial region were considered for the spent fuel analysis. The burnup of the spent fuel was set at 40 MWd/kgHM, with a cooling time of 20 years [5].

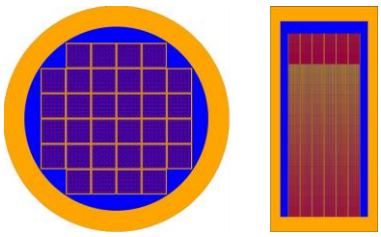

Fig. 2. Configuration of GBC-32 cask modeled with Serpent2

Table II. Dimensional information of GBC-32 cask

Parameters	
Cell inside/outside radius	11.0 cm/11.75 cm
Cell wall thickness	0.75 cm
Boral Al plate thickness	0.25 cm
Cell pitch	24.0 cm
Cell & boral plate height	381 cm
Cask inside/outside radius	87.5 cm/107.5 cm
Cask inside/outside height	390 cm/450 cm

3. Results

3.1. Single fuel assembly with boundary conditions

First, as shown in **Table III**, we performed calculations on a 2D single assembly using both reflective and vacuum boundary conditions. The calculation options were set to 200,000 particles, with 200 active cycles and 100 inactive cycles.

As shown in **Table IV**, under the reflective condition, the multiplication factor with S(α,β) was lower than the one without S(α,β) . In contrast, under the vacuum condition, we observed that the multiplication factor increased when S(α,β) was applied. In particular, it is noted that the increase in multiplication factor using S(α,β) is very large for the case using vacuum B.C. while the change for the reflective B.C. case was relatively small.

Table III. Calculation option of Serpent2 and MCNP6

Calculation option	
Number of neutron particles	200,000
Number of active cycles	200
Number of inactive cycles	100
Boundary conditions	Reflective / Vacuum

Table IV. Multiplication factors of 2D single FA under reflective, vacuum B.C. calculated by Serpent2 and MCNP6 and standard deviation (multiplication factor)

	Reflective (k_{inf})	**Vacuum (k_{eff})**	**Standard deviation**
	Values (Serpent2/MCNP6)		
Without S(α,β)	1.41776 /1.41818	0.79168 /0.79151	0.00006 /0.00011
With S(α,β)	1.41467 /1.41515	0.79868 /0.79814	0.00006 /0.00010
Difference in reactivity (pcm)	154/150	1107/1050	-

3.2. 2D single fuel assembly with P/D ratio

Secondly, to analyze the effects of S(α,β) in more detail, we examined its impact by varying the P/D ratio of the FA. We conducted calculations by adjusting the water region, which significantly affects thermal scattering, while keeping the fuel region unchanged. The boundary conditions were the same as in the first calculation, using both reflective and vacuum conditions. As shown in Fig. 3, under reflective conditions, the multiplication factor was lower for all calculated P/D ratios when S(α,β) was applied. Additionally, we observed that the difference between the calculations increased as the moderation region expanded. **Fig. 4** shows that under vacuum conditions, in the under-moderation region, calculations with S(α,β) applied resulted in higher multiplication factors, while in the over-moderation region, they were lower. Moreover, in the over-moderation region, the difference between the two calculations increased as the moderation region expanded. As expected, these results mean that the influence of S(α,β) becomes more pronounced as the amount of water increases.

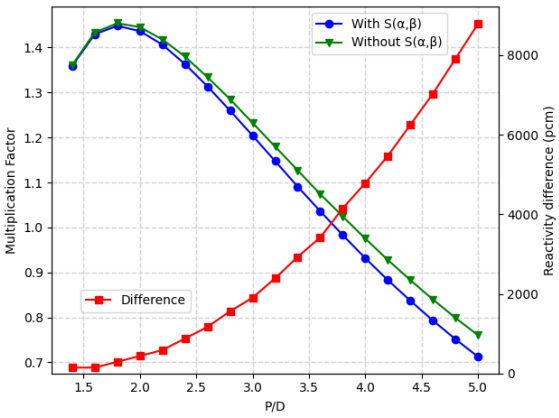

Fig. 3. Changes in multiplication factor according to P/D ratio and their differences under reflective B.C.

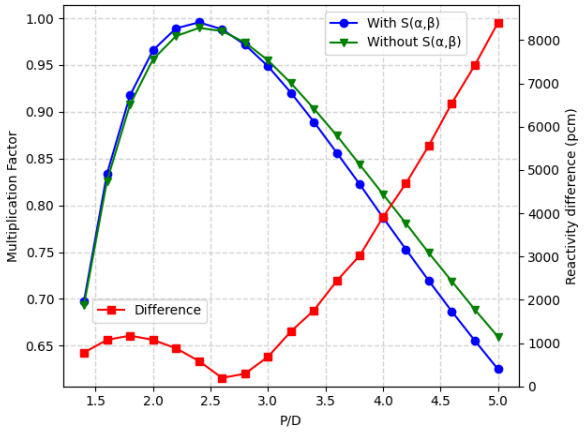

Fig. 4. Changes in multiplication factor according to P/D ratio and their differences under vacuum B.C.

To verify the calculations in this study, we performed same computations using MCNP6. As shown in **Table V**, when comparing the results of Serpent2 and MCNP6 under reflective boundary conditions, the differences between the two codes were less than 40pcm in all cases. Although not explicitly included in Table V, we confirmed that for other cases as well, the differences in calculation results between Serpent2 and MCNP6 were all within 100pcm. Based on these results, we concluded that the calculations performed in this study have sufficient reliability.

Table V. Difference (pcm) between Serpent2 and MCNP6 with P/D ratio under reflective B.C. and standard deviation (multiplication factor)

P/D ratio	S(α, β)	Normal	Standard deviation (Serpent2/MCNP6)
	Difference (pcm)		
1.6	33	28	0.00006/0.00011
2.0	29	11	0.00005/0.00010
2.4	3	8	0.00006/0.00010
2.8	1	3	0.00006/0.00009
3.2	10	5	0.00009/0.00011
3.6	2	39	0.00009/0.00010
4.0	1	1	0.00011/0.00011
4.4	14	33	0.00013/0.00012
4.8	18	27	0.00015/0.00012

3.3. GBC-32 cask criticality calculation

Finally, we calculated how S(α,β) affects the multiplication factor in the GBC-32 cask criticality evaluation. The calculation options were kept the same as in the previous calculations.

As shown in **Table VI**, in the GBC-32 cask criticality evaluation, the use of S(α,β) was shown to reduce the multiplication factor. The difference in k_{eff} was 1141 pcm between the cases with S(α,β) and without S(α,β). This phenomenon appears to be due to the large moderation region inside the GBC-32 cask.

Table VI. Calculation result of GBC-32 cask under vacuum condition (Serpent2)

	k_{eff}
Without S(α,β)	0.78594 (±0.00008)
With S(α,β)	0.77895 (±0.00008)
Difference in reactivity (pcm)	1141

4. Conclusions

In this study, we evaluated the impact of the S(α,β) on criticality evaluations using 2D assembly models and 2D assembly calculations with various P/D ratios. From the results, it was found that the influence of the S(α,β) thermal scattering law generally increased as the

moderation region (water region) expanded. To ensure the reliability of these calculations, we performed verification calculations using MCNP6. The difference in multiplication factors between Serpent and MCNP6 was mostly within 40 pcm.

Additionally, to evaluate the effect of the S(α,β) thermal scattering law on cask criticality calculations, we modeled the GBC-32 cask and performed criticality calculations, which showed that the multiplication factor decreased by 1141pcm when the S(α,β) was applied.

Acknowledgment

This work is financially supported by the Korea Institute of Energy Technology Evaluation and Planning (KETEP) grant funded by the Ministry of Trade, Industry and Energy (MOTIE) of Republic of Korea (No. RS-2024-00398867).

REFERENCES

[1] U.S. NRC (U.S. Nuclear Regulatory Commission). 2020. "Chapter 7 - Criticality Evaluation." In Standard Review Plan for Spent Fuel Dry Storage Systems and Facilities, NUREG-2215. Washington, DC: U.S. Nuclear Regulatory Commission.
[2] Leppänen, J. (2015). Serpent – a Continuous-energy Monte Carlo Reactor Physics Burnup Calculation Code: User's Manual. VTT Technical Research Centre of Finland. June 18, 2015.
[3] J. T. Kulesza, B. C. Kiedrowski, C. J. Werner, et al., "MCNP® Code Version 6.3.0 Manual," LA-UR-22-30006, Rev. 1, Los Alamos National Laboratory (2022).
[4] W. A. Wieselquist, R. A. Lefebvre, and M. A. Jessee, Eds., "SCALE Code System," ORNL/TM-2005/39, Version 6.2.4, UT-Battelle, LLC, Oak Ridge National Laboratory (2020).
[5] Yun, H., Park, K., & Hong, S. G. (2016). A Criticality Analysis of the GBC-32 Dry Storage Cask with Hanbit Nuclear Power Plant Unit 3 Fuel Assemblies from the Viewpoint of Burnup Credit. Nuclear Engineering and Technology, 48(3), 624-632.